

# Thermocapillary Migration of Liquid Droplets Induced by a Unidirectional Thermal Gradient

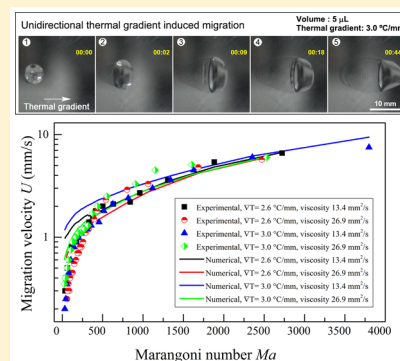
Qingwen Dai,<sup>†,§</sup> M. M. Khonsari,<sup>‡</sup> Cong Shen,<sup>‡</sup> Wei Huang,<sup>†</sup> and Xiaolei Wang<sup>\*,†,§</sup>

<sup>†</sup>College of Mechanical and Electrical Engineering, Nanjing University of Aeronautics & Astronautics, Nanjing 210016, China

<sup>‡</sup>Department of Mechanical and Industrial Engineering, Louisiana State University, 2508 Patrick Taylor Hall, Baton Rouge, Louisiana 70803, United States

<sup>§</sup>Jiangsu Key Laboratory of Precision and Micro-Manufacturing Technology, Nanjing 210016, China

**ABSTRACT:** A liquid droplet placed on a nonuniformly heated solid surface will migrate from a high-temperature region to a low-temperature region. This study reports the development of a theoretical model and experimental investigation on the migration behavior of paraffin oil droplets induced by the unidirectional thermal gradient. Thin-film lubrication theory is employed to determine the migration velocity of droplets, and temperature dependence of viscosity is taken into account. Comparisons between experimental and numerical results are presented. An effective approach for estimating the thermocapillary migration velocity of droplets on lubrication is proposed.



## 1. INTRODUCTION

In tribo-system, a process involving friction is always accompanied by a dissipation of energy, which generates heat and forms a thermal gradient on the rubbing surfaces.<sup>1</sup> Naturally, the generated thermal gradient yields some interesting and complex thermodynamic behavior associated with the migration of the lubricant. A liquid lubricant can be driven by thermal gradients to flow from a high-temperature region to a low-temperature region.<sup>2–6</sup>

Typically, the existence of thermal gradients induces an interfacial tension gradient at the liquid–gas surface, creating a tangential stress at that surface. Consequently, convective currents inevitably arise in the liquid, and the migration commences shortly thereafter.<sup>7–10</sup> The study of the migration of droplets and the investigation of the influence of external temperature fields is a research area of fundamental importance in many industrial products such as miniature rolling bearings, hard disk, microelectronics, and so on.<sup>11–14</sup> In the case of lubricant droplets on stainless steel there is a continual drainage, and the thermal flow seriously affects the behavior of the lubrication and causes potential lubrication failure. Research is thus needed to better understand the nature of liquid droplet migration.

Over the past decade, abundant experimental and theoretical investigations have been performed on the thermocapillary migration.<sup>15–18</sup> Many of the experimentally developed strategies including the geometrical anisotropy,<sup>19–21</sup> wettability gradients,<sup>22</sup> low surface energy coating,<sup>23</sup> and idiosyncratic lubricant<sup>24</sup> can be put to use to effectively regulate the liquid migration on a surface. Mechanistically, when placed on a surface, a liquid droplet either migrates or contracts<sup>25</sup> to an

equilibrium shape in which the capillary and hydrostatic pressure fields are balanced inside the droplet. Greenspan<sup>26</sup> reported the development of a 2D model to describe the motion of a small viscous droplet wetting a surface. He incorporated both capillary and viscous forces within the context of the lubrication theory and applied the dynamic contact angle to describe the forces acting on the fluid at the contact line. Making use of this model, Ehrhard and Davis<sup>27</sup> studied the spreading of a viscous liquid droplet on a uniformly heated or cooled smooth horizontal surface but without a thermal gradient on that surface. Brochard<sup>28</sup> and Brzoska et al.<sup>29</sup> studied the spreading characteristics of several given shape droplets induced by either chemical or thermal gradients. Using the thin-film lubrication theory, they reported results for the spreading velocity via the balance between local viscous force and energy. Ford et al.<sup>30</sup> investigated the thermocapillary migration of droplets having an arbitrary height profile on a surface imposed with a uniform temperature gradient. Subramanian et al.<sup>31</sup> further developed a theoretical analysis that considered the 3D axisymmetric spherical-cap shape of small droplet migrating on a wettability gradient surface. These contributions to this field provide valuable insights into the understanding of this complex phenomenon.

A 2D model is set up to derive the migration velocity of a liquid droplet on a surface with a unidirectional thermal gradient. We derive an evolution equation for the interface viscous force resisting the unbalanced Young force that

Received: April 28, 2016

Revised: July 6, 2016

Published: July 11, 2016

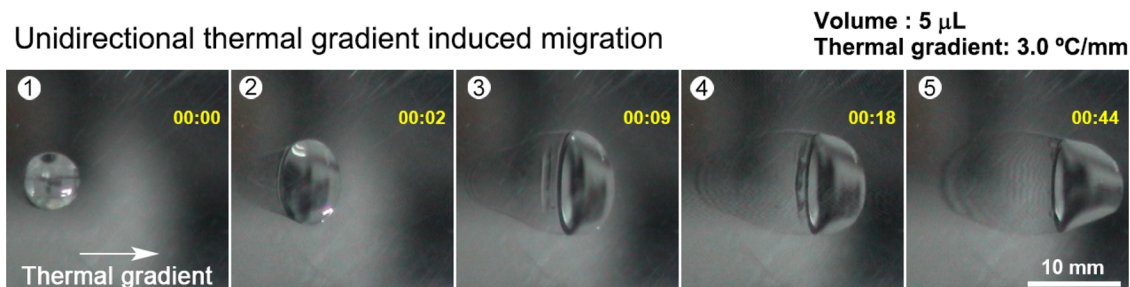


**Figure 1.** Thermo-capillary migration of paraffin oil droplet on the smooth surface induced by a unidirectional thermal gradient.

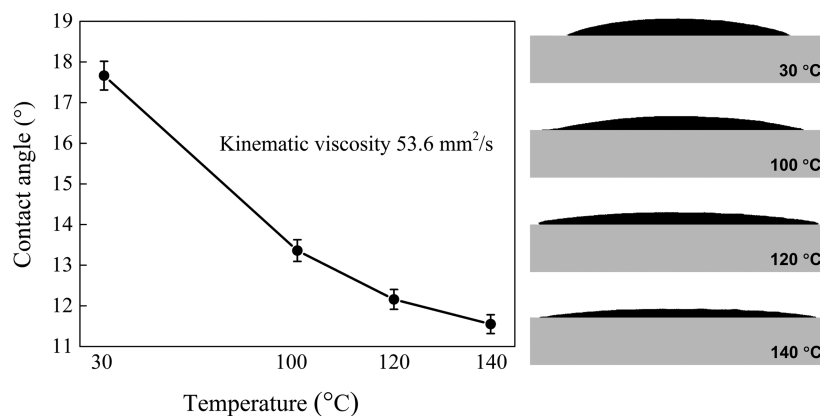


**Figure 2.** Equilibrium contact angle of paraffin oil at various temperatures.

accounts for the migration and present experimental results evidence of the validity of the approach.

Proper consideration of the lubricant migration in engineering applications requires taking the temperature dependence of lubricant viscosity into account. The previous experimental result reveals that under a unidirectional thermal gradient the droplet of paraffin oil tends to migrate from the high-temperature region to a low-temperature region (i.e., from left to right), and more importantly, accompanied by a diffusion process, as shown in Figure 1. Because a liquid lubricant viscosity tends to decrease (or, alternatively, its fluidity tends to increase) as its temperature increases, the variation in viscosity induced by temperature should be taken into consideration in the theoretical analysis.

Hence, we report the results of experimental and theoretical study of the thermocapillary migration of a liquid droplet on a metal substrate surface. The temperature dependence of lubricant viscosity is taken into account. In the analysis, we predict the migration velocity on the surface with a unidirectional thermal gradient and provide an effective approach for the valuation of migration velocity.

## 2. ANALYSIS

The geometric features of the droplet have a significant influence on the theoretical model. The equilibrium contact angle of the paraffin oil with a kinematic viscosity of 53.6  $\text{mm}^2/\text{s}$  was measured at various temperatures to develop a realistic cross-sectional shape of a droplet. The measurement is based on the static sessile drop method, and the value is often quite close to the advancing contact angle. As shown in Figure 2, increasing the temperature leads to a rapid decrease in contact angle and the droplet is almost flattened as the temperature is increased to 140  $^{\circ}\text{C}$ , forming a pancake-shaped configuration. For the paraffin oil, the contact angle decreases significantly

with the decreasing viscosity. In fact, at high temperatures ( $>100$   $^{\circ}\text{C}$ ), the contact angles of the paraffin oils with lower kinematic viscosities become too small to be measured with precision. Therefore, it is believed that the height of the droplet is considerably less than its width, and the radius of the droplet grows beyond the capillary length ( $L_C = \sqrt{\gamma/\rho g}$ ). The droplet transforms to a pancake-shaped configuration, that is, a thin film, and it is curved only at the rim. We ignore the variation of the contact angle induced by the thermal gradient, regarding it as a small constant value.

The temperature dependence of liquid viscosity describes the phenomenon that liquid viscosity tends to decrease as its temperature increases. A well-known exponential model for the relationship between the temperature and viscosity is employed to calculate the viscosity<sup>32</sup>

$$\mu(T) = \mu_0 e^{-b(T-T_0)} \quad (1)$$

where  $\mu$  is the viscosity,  $\mu_0$  is the viscosity at the reference temperature,  $T$  is the temperature and  $T_0$  is the reference temperature of the liquid, and  $b$  represents the viscosity temperature coefficient.

The thermal gradient is considered as a constant value,  $\frac{\partial T}{\partial x} = \text{const} = C_T$ , because the droplet film is extremely thin, the height dependence of viscosity is ignored, and the temperature dependence of viscosity in the migration direction is taken into consideration, as a function of position  $x$  of the droplet

$$\mu(x) = \mu_0 e^{-b[(T_S - C_T x) - T_0]} \quad (2)$$

where  $T_S$  is the temperature at the start position, referenced to the droplet, and it is defined at the trailing edge of the droplet.

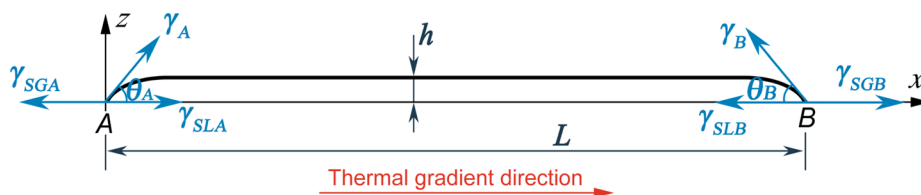


Figure 3. Side view of a droplet film on the ideal surface.

In the following analysis, the thin-film lubrication theory is employed to predict the migration velocity of the droplet. The quasisteady condition is assumed based on the work of Pratap et al.,<sup>33</sup> who demonstrated that the temperature-induced motion of a drop on a surface can be reliably modeled as a quasisteady process. This implies that for the droplet placed at a given location the time taken for the temperature to stabilize is shorter than that required for the droplet to move an appreciable distance from that location. The temperature of the droplet will be in equilibrium with that of the substrate surface. The motion of the droplet under a thermal gradient is governed by the balance of two forces acting on the droplet ridge: The viscous resistance force ( $F_v$ ) and the driving force ( $F_d$ ), which is directly related to the gradients of the liquid–gas interfacial tension.<sup>34,35</sup> We now proceed to derive the governing equations of the forces under a unidirectional thermal gradient.

We consider the case of a 2D droplet of oil placed on a horizontal and impermeable surface with a constant thermal gradient. Having specified the positions of the droplet at points A and B, a Cartesian coordinate system is set up to determine the positions of the droplet as the migration progresses. This information is needed to calculate the local temperature and viscosity. The side view of the section is shown in Figure 3, the height of the droplet is  $h$ , and the width is  $L$ . The velocity in the droplet is governed by the Navier–Stokes and the continuity equations

$$\frac{D\mathbf{V}}{Dt} = \mathbf{F} - \frac{1}{\rho}\nabla\mathbf{P} + \frac{\mu}{\rho}\nabla^2\mathbf{V} \quad (3)$$

$$\nabla\mathbf{V} = 0 \quad (4)$$

where  $\mathbf{V}$  is the flow velocity,  $\mathbf{F}$  is the inertial force,  $\mathbf{P}$  is the pressure field,  $\rho$  is the density of the liquid, and  $\mu$  is the dynamic viscosity.

For the thermocapillary migration, the velocity is very slow (creeping motion), the viscous force dominates the inertial forces, and the thin-film lubrication approximation applies. Assuming  $\mu = \mu(x)$ , eq 3 reduces to

$$\frac{\partial P}{\partial x} = \mu(x) \frac{\partial^2 V_x}{\partial z^2} \quad (5)$$

We select a reference frame traveling with the droplet so that the droplet can be regarded as stationary and the substrate moves in the negative  $x$  direction with a constant speed  $U$ . The boundary conditions at  $z = h(x)$  and  $z = 0$  are

$$\begin{cases} \frac{\partial V_x}{\partial z} = \frac{1}{\mu(x)} \frac{\partial \gamma}{\partial x}, & z = h(x) \\ V_x = -U, & z = 0 \end{cases} \quad (6)$$

where  $\gamma$  is the surface tension of the liquid.

Integrating eq 5, applying the boundary conditions, and solving for the velocity field, we have

$$V_x(z) = \frac{1}{\mu(x)} \left[ C_T \gamma_T z + \frac{1}{2} \frac{\partial P}{\partial x} (z^2 - 2zh) \right] - U \quad (7)$$

where  $\gamma_T$  represents the surface tension coefficient,  $\gamma_T = \frac{\partial \gamma}{\partial T}$ .

In the frame of moving reference, the droplet travel distance is assumed to be small. There is no volumetric flux passing through the vertical cross-section of the droplet. Therefore

$$\int_0^h V_x(x, y, z) dz = 0 \quad (8)$$

The pressure gradient satisfying this constraint is given by

$$\frac{\partial P}{\partial x} = -\frac{3\mu(x)}{h^2} U + \frac{3}{2h} C_T \gamma_T \quad (9)$$

Combining eqs 7 and 9, the viscous stress  $\sigma_{xz}$  at the solid–liquid interface can be written as

$$\sigma_{xz}(z=0) = \mu(x) \left( \frac{\partial V_x}{\partial z} \Big|_{z=0} \right) = \frac{3\mu(x)}{h} U - \frac{1}{2} C_T \gamma_T \quad (10)$$

Ignoring the change in the thickness at the rim of the thin film, that is,  $h$  is constant between positions A and B (see Figure 3), the viscous resistance force  $F_v$  can be finally obtained as

$$F_v = \int_{x_A}^{x_B} \sigma_{xz}(z=0) dx = g(x_A, x_B) \frac{3\mu_0}{h} U - \frac{1}{2} \gamma_T C_T L \quad (11)$$

where

$$g(x_A, x_B) = \frac{1}{bC_T} (e^{b(C_T x_B - T_S + T_0)} - e^{b(C_T x_A - T_S + T_0)}) \quad (12)$$

Next, we estimate the driving force exerted on the droplet. For a sessile droplet placed on a surface, the Young's equation defines the interfacial tension force balance and contact angle in the vicinity of three-phase contact line<sup>36</sup>

$$\gamma_{SG} = \gamma_{SL} + \gamma \cos \theta \quad (13)$$

where  $\gamma_{SG}$  and  $\gamma_{SL}$  are the solid–gas and solid–liquid interfacial tensions, respectively.

The unbalanced Young force, generating the driving force ( $F_d$ ) on the droplet, can be written as

$$F_d = (\gamma_{SG} - \gamma_{SL})_B - (\gamma_{SG} - \gamma_{SL})_A \quad (14)$$

The surface tension relationship between positions A and B (see Figure 3) along the footprint of the droplet can be described as

$$\gamma = \gamma_0 + \frac{\partial \gamma}{\partial x} x = \gamma_0 + C_T \gamma_T x \quad (15)$$

where  $\gamma_0$  is the reference surface tension of the liquid.

Combining eqs 13–15, we arrive at the following equation for the driving force  $F_d$

$$F_d = \gamma_T C_T L \cos \theta \quad (16)$$

The force acting on the droplet under the unidirectional thermal gradient is deduced from a balance between the driving force and the viscous force that resists it ( $F_d = F_v$ )

$$\gamma_T C_T L \cos \theta = g(x_A, x_B) \frac{3\mu_0}{h} U - \frac{1}{2} \gamma_T C_T L \quad (17)$$

Therefore, the migration velocity can be described by the following relationship

$$U = \frac{1}{g(x_A, x_B)} \frac{(2 \cos \theta + 1) \gamma_T C_T L}{6\mu_0} \frac{Q}{S} \quad (18)$$

where  $Q$  is the volume of the droplet film and  $S$  is the area of the liquid. Both of them can be measured during a test.

The migration velocity ( $U$ ) is calculated and compared with the experimental results in the following sections. The area ( $S$ ) is varying due to diffusion and viscous effects as the droplet migrates along the surface. We measured the area of the liquid during the migration process in each frame and utilized the calculated value of  $h$  in the analysis. This procedure for predicting the migration velocity significantly improves the results and makes the prediction more reasonable than assuming a constant  $h$  throughout. Because the contact angle of the paraffin oils employed for the migration test is small and difficult to measure, during the theoretical calculation, the value of  $\cos \theta$  is assumed to be 1.

### 3. EXPERIMENTAL SECTION

Figure 4 shows the schematic diagram of the experimental apparatus used in this study. Migration was performed on the rectangular

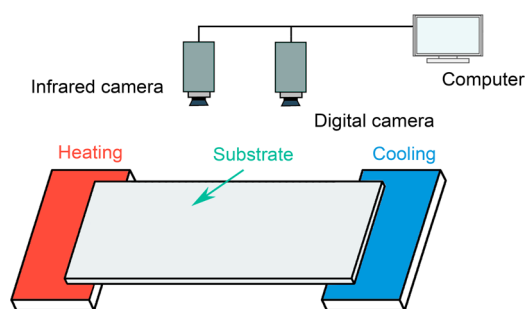


Figure 4. Schematic diagram of the experimental apparatus.

substrate surface with dimensions of 76 mm × 30 mm × 3 mm. All substrates were made of SUS 316 stainless steel with an average surface roughness  $R_a$  of 0.02  $\mu\text{m}$ . Heating and cooling elements were designed to generate a unidirectional thermal gradient on the substrate surface. The cooling element was maintained at a constant temperature of 0  $^{\circ}\text{C}$ . By setting the temperature of the heating one to 120 and 138  $^{\circ}\text{C}$ , thermal gradients of 2.6 and 3.0  $^{\circ}\text{C}/\text{mm}$  were generated along the length of the surface, respectively. A thermal imaging acquisition device was employed to obtain the temperature gradient map on the surface. The more detailed description of the apparatus was given in our previous paper; see ref 21.

A digital video camera was used to monitor the dynamic migration process to obtain quantitative experimental results. Via extracting the frames during the migration process, the area ( $S$ ) of the film and the migration distance (measured at the front edge of the droplet) were obtained. Then, the mean migration velocity and droplet height were calculated.

Paraffin oil is a mixture of liquid hydrocarbons obtained from fractionation of the atmospheric distillation of petroleum. It is a

common base oil for lubricant, and, most importantly, there are fewer additives in this oil and thus their influence on the migration behavior can be ruled out. Therefore, paraffin oils with different kinematic viscosities were chosen for the experiments in this study. The viscosities were measured with an Ubbelohde viscometer, a capillary-based viscosity measurement device. The surface tension of the lubricants was measured using the Wilhelmy plate method. By measuring the surface tensions of the lubricants at various temperatures, the mean surface tension coefficient was obtained and used in the numerical calculations.

Prior to each test, the substrates were ultrasonically cleaned with acetone and ethanol and blow-dried with nitrogen. Paraffin oils with various kinematic viscosities were used in the migration experiments, and the initial temperature of all tested paraffin oils was room temperature ( $\sim 25$   $^{\circ}\text{C}$ ). The dosage of the droplet was kept as a constant value of 5  $\mu\text{L}$  via a microliter syringe. The main physical parameters of paraffin oils are listed in Table 1.

Table 1. Physical Parameters of Paraffin Oil at 40  $^{\circ}\text{C}$

parameter	paraffin oil-1	paraffin oil-2
kinematic viscosity ( $\text{mm}^2/\text{s}$ )	13.4	26.9
density ( $\text{g}/\text{cm}^3$ )	0.82904	0.8322
surface tension coefficient ( $\text{mN}/(\text{m } ^{\circ}\text{C})$ )	0.082	0.081
specific heat capacity ( $\text{J}/(\text{kg } ^{\circ}\text{C})$ )	2650	2700
thermal conductivity $\text{W}/(\text{m } ^{\circ}\text{C})$	0.337	0.341
viscosity temperature coefficient	0.02414	0.02984

### 4. RESULTS AND DISCUSSION

Figure 5 shows the viscosity–temperature correlation of the paraffin oils. The kinematic viscosities were measured at eight

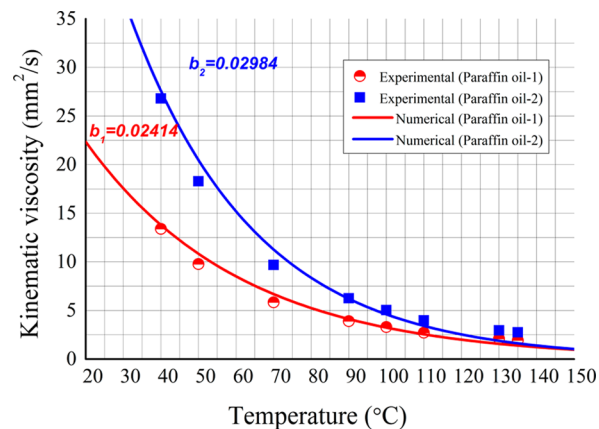
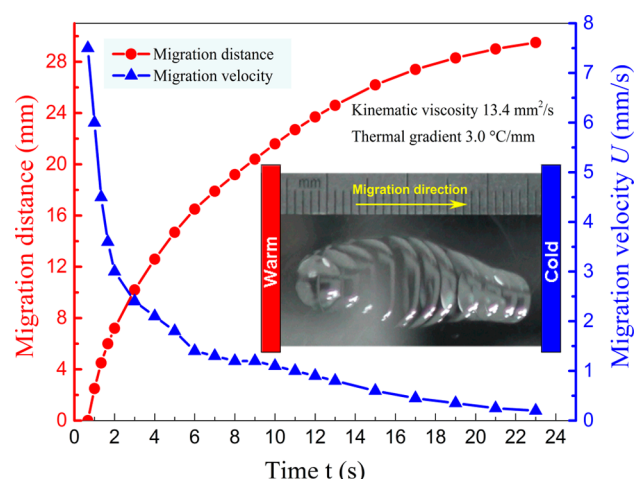


Figure 5. Viscosity–temperature correlation of these paraffin oils.

different temperatures. It can be seen that the kinematic viscosity of paraffin oil decreases with increasing temperature. It is known that the liquid density changes with temperature and pressure. In general, the density decreases slightly with increasing temperature under the atmospheric pressure.<sup>37</sup> While in the temperature range varying from 30 to 140  $^{\circ}\text{C}$  the viscosity drops dramatically, the density change is very small and can be neglected. Experimental data for two paraffin oils were fitted to eq 1 and utilized in the theoretical analysis to account for the variation of viscosity as a function of temperature.

In the following section, experiments on the migration of droplets under unidirectional thermal gradients and the comparison with numerical results are conducted. Figure 6





**Figure 6.** Migration distance and velocity of a paraffin oil with a kinematic viscosity of  $13.4 \text{ mm}^2/\text{s}$  versus elapsed time under a thermal gradient of  $3.0 \text{ }^\circ\text{C}/\text{mm}$  and the detailed dynamic migration process.

shows the migration distance and velocity of a paraffin oil droplet with an initial kinematic viscosity of  $13.4 \text{ mm}^2/\text{s}$  under a thermal gradient of  $3.0 \text{ }^\circ\text{C}/\text{mm}$ , plotted as a function of time. Initially, the migration distance increases very quickly, and the migration velocity is fast. With time elapsing, the increment of migration distance becomes inconspicuous, while the migration velocity begins to decrease and finally diminishes close to zero.

The inset image in Figure 6 exhibits the detailed dynamic migration process of the droplet; it is a superimposed image composed of key video frames. The migration progresses from the warm region to the cold region. An interesting phenomenon occurring with the migration process is that the droplet spreads in the width direction of the substrate and then contracts back to the droplet shape. This trend can be explained as follows. It is known that an oil droplet is more prone to spread on a heated surface. Initially, because the temperature of the starting position is quite high, the migration occurs by spreading in the width direction; however, as the temperature of the droplet decreases during the migration process, the viscosity and liquid–gas interfacial tension of the droplet increase. Consequently, the diffusion process in width direction is obstructed, and the liquid tends to contract as it approaches the cold region.

Figure 7 presents the comparison between the experimental and numerical results of migration velocity. Paraffin oil with a kinematic viscosity of  $13.4 \text{ mm}^2/\text{s}$  was tested under the thermal gradients of 2.6 and  $3.0 \text{ }^\circ\text{C}/\text{mm}$ . Migration velocity is plotted as a function of position  $x$ , that is, the location of the front edge of the droplet. Referring to Figure 7a, the beginning migration velocity is  $\sim 6.6 \text{ mm/s}$ , and it decreases rapidly as the migration continues. The line graph shows the numerical result of the migration velocity. Note that the predicted velocity results are in accordance with the experimental data both in trend and in magnitude: It first rapidly decreases from a high value to a low value and then decreases to zero gradually. The numerical data agree quite well with the experimental result at the beginning, and a slight difference exists with increasing migration distance. Figure 7b presents the comparison between the experimental and numerical results under a thermal gradient of  $3.0 \text{ }^\circ\text{C}/\text{mm}$ . It can be observed that at the beginning, the migration velocity increases to  $7.5 \text{ mm/s}$ ; compared with Figure 7a, an increasing thermal gradient clearly increases the migration velocity. The

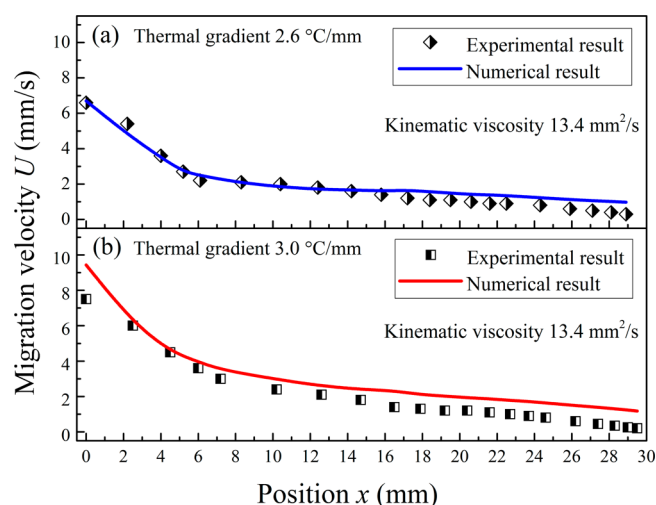


**Figure 7.** Comparison between the experimental and numerical results of migration velocity  $U$ , with a paraffin oil of a kinematic viscosity of  $13.4 \text{ mm}^2/\text{s}$  under a thermal gradient of (a) 2.6 and (b)  $3.0 \text{ }^\circ\text{C}/\text{mm}$ .

trends of numerical results under these two thermal gradients are consistent with the experimental data.

Figure 8 presents the comparison between the experimental and numerical results with another kind of paraffin oil, with a

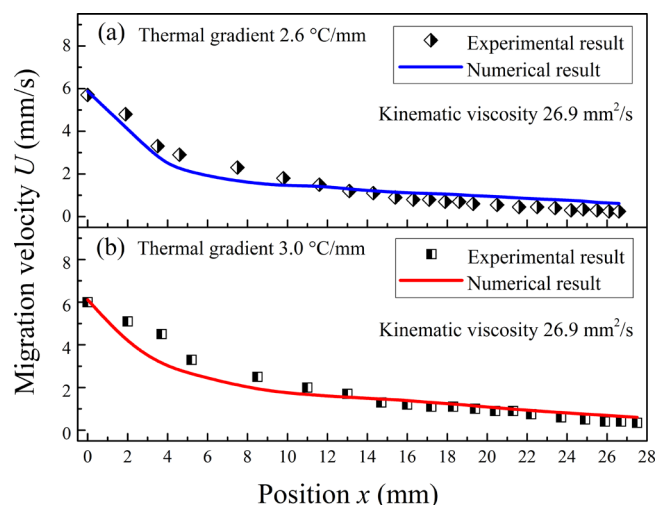


**Figure 8.** Comparison between the experimental and numerical results of migration velocity  $U$  with a paraffin oil of a kinematic viscosity of  $26.9 \text{ mm}^2/\text{s}$  under a thermal gradient of (a) 2.6 and (b)  $3.0 \text{ }^\circ\text{C}/\text{mm}$ .

higher initial kinematic viscosity of  $26.9 \text{ mm}^2/\text{s}$ , under thermal gradients of 2.6 to  $3.0 \text{ }^\circ\text{C}/\text{mm}$ . Compared with Figure 7, it can be noted that under the same thermal gradient the migration velocity decreases with increasing initial viscosity. The migration velocities of experimental and numerical results show a very similar trend: They both decrease quickly at first and then gradually approach zero. More importantly, the numerical results are in good agreement with the experimental data.

As noted by Brochard,<sup>28</sup> a variety of models have been proposed to derive the profile of the moving droplets. The equilibrium shape of a liquid droplet placed on a horizontal solid surface is controlled by the spreading coefficient, and under certain conditions, the simplification of the droplet as a thin pancake is reasonable. When the liquid spreads to form a

thin pancake, the deformation of the droplet shape during the migration can be neglected, and one can assume a quasisteady equilibrium and the predicted velocity turns out to be proportional to the thickness. This relationship is consistent with our theoretical derivations.

In this study, the initial temperature of all of the tested droplets is room temperature ( $\sim 25^\circ\text{C}$ ), and to simplify the analysis we have assumed that the droplet reaches the surface temperature as soon as it hits the surface; however, this initial temperature can potentially play an important role in the initial acceleration phase, affecting the migration velocity.

Wasan et al.<sup>38</sup> pointed out that the thermal gradient yielded migration velocity can be treated as a constant value, with regarding the viscosity of droplet as an invariant parameter; however, our experimental results show a decreasing trend of migration velocity during the migration process. When taking the viscous dissipation into consideration, it is of importance to take the temperature dependence of viscosity into account if the viscosity changes rapidly with the temperature. Referring to eq 18, the viscosity is not constant, and its variation significantly influences the migration velocity. Because the local temperature of the droplet decreases with the migration process, the viscosity of the droplet increases and the migration velocity keeps decreasing in the  $x$  direction gradually. This is the reason that the migration velocity decreases rapidly in the beginning and then slows down to zero. Moreover, eq 18 indicates that the migration velocity is inversely proportional to the initial viscosity. Therefore, as shown in Figures 7 and 8, increasing the initial viscosity from 13.4 to 26.9  $\text{mm}^2/\text{s}$  yields a reduction in the migration velocity (under a thermal gradient of  $3.0^\circ\text{C}/\text{mm}$ , the initial value decreases from 7.5 to 6.0  $\text{mm}/\text{s}$ ). Meanwhile, according to eq 18, the thermal gradient is also an influential parameter in predicting the velocity, and the numerical value is proportional to the thermal gradient. The results shown in Figures 7 and 8 verify the fact that migration velocity increases with increasing the thermal gradient.

In the analytical model, the migration surface is assumed to be completely smooth. Our previous research<sup>39</sup> revealed that the migration velocity decreases with decreasing surface roughness under certain conditions and the differences tend to disappear with the further decreasing of surface roughness. In this study, the thickness of the droplet film is  $\sim 100\ \mu\text{m}$ , while the testing surface, with an average surface roughness  $R_a$  of  $0.02\ \mu\text{m}$ , is smooth enough when compared with the film thickness. Therefore, in this study the effect of surface roughness was not considered; however, if the lubricant film thickness is as small as the magnitude of the surface roughness, the surface roughness effect would be a significant influence factor.

The predicted migration velocities in Figures 7 and 8 agree well with the experimental data both in trend and in magnitude; however, slight differences exist that can be explained as follows. First, the current model ignores the rim of the droplet film, and the contact angle is considered to be nil in the calculation. Moreover, the relationship in eq 5 assumes that viscosity is constant in thickness direction, that is,  $\mu \neq \mu(z)$ . These assumptions may, in part, be responsible for differences between the prediction and the experimental results. Second, the migration velocity is also inversely proportional to the area of the droplet ( $S$ ). Referring to Figure 6, as the trajectory of a droplet on the surface with the unidirectional thermal gradient shows, the migration occurs with a diffusion-and-constriction process, leaving minute residual oil on its trajectory. Therefore,

the variation of droplet area and volume can have a major influence on the migration velocity.

Additionally, we consider the effect of surface tension at the leading and trailing edges of the liquid droplet by developing a 2D model. The 2D assumption makes the prediction relatively easy to realize. Clearly, the surface tension force and viscous resistance force are the dominant forces acting on the droplet. In a 3D world, not only does the surface tension translate to a circle, that is, the circumference of the droplet, but also the viscosity force is translated. These would partially offset the error induced by the simplification of the 2D model. We thus believe that the results of the simplified 2D model are reasonable. Nevertheless, more accurate results are expected with a 3D model.

In all experiments, the migration occurs from warm to cold regions. The thermal gradient on the liquid film will change the surface tension of the fluid, creating imbalance in equilibrium. The induced thermo-capillary forces will pull the liquid from warmer to cooler regions until equilibrium is established. The Marangoni number ( $Ma$ ) is a dimensionless number proportional to surface tension forces (thermal gradient induced) divided by viscous forces.<sup>40,41</sup> It can be used to characterize the relative effects of surface tension and viscous forces. It is defined as

$$Ma = \frac{\gamma_T T_\Delta h}{\mu \kappa} \quad (19)$$

where  $\kappa$  is the thermal diffusivity, which is the thermal conductivity divided by density and specific heat capacity at constant pressure, and  $T_\Delta$  is a characteristic temperature difference across the droplet layer. Because we assume that the droplet reaches the surface temperature as soon as it hits the surface, we define the  $T_\Delta$  as the temperature difference between lowest and highest layer of the droplet, that is, the temperature on substrate surface where the droplet located and the room temperature.

Combining eqs 18 and 19, we can finally arrive at the following relationship between the migration velocity ( $U$ ) and the Marangoni number ( $Ma$ )

$$U = \frac{(2 \cos \theta + 1) LC_T \kappa}{6 T_\Delta} \cdot Ma \quad (20)$$

Using this equation, we plot all experimental and numerical migration velocities as a function of the Marangoni number, as shown in Figure 9. It can be seen that the migration velocity increases with the increasing Marangoni number. When the Marangoni number is small, some differences exist between the experimental and numerical results. With the increasing Marangoni number, almost all data of different experimental conditions are consistent with each other and fit the numerical results well, and even if the experimental conditions are different, the same migration velocities are achieved under the same value of Marangoni number. Referring to the definition of Marangoni number (surface tension forces divided by viscous forces), a higher value of Marangoni number means that the surface tension forces play a dominate role, and the driving force is remarkably larger than the viscous resistance force, which makes the above-mentioned influence factors far less important. Therefore, the migration velocity trends reach unanimity. This agreement further establishes the validity of the theoretical analysis.

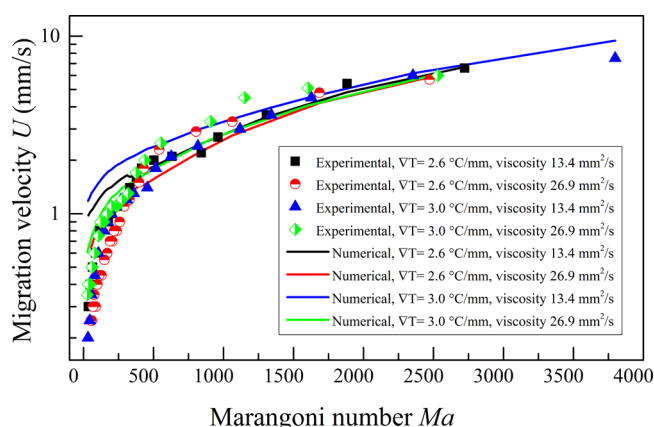


**Figure 9.** Experimental and numerical migration velocities versus the Marangoni number on the smooth surface with different viscosities and thermal gradients.

## 5. CONCLUSIONS

Experimental and theoretical studies are carried out to investigate the migration behavior of lubricant droplet induced by the unidirectional thermal gradient. An analytical model is developed, and its prediction is compared with experimental results. The conclusions drawn from this study are as follows:

1. An analytical approach using the thin-film lubrication equation with a temperature-dependent viscosity is proposed for the prediction of migration velocity of droplets.
2. The numerical results show good agreements with the trends of experimental data: The migration velocity decreases quickly at first and then approaches to zero gradually, and its magnitude increases with increasing thermal gradient or decreasing initial viscosity.
3. For industrial applications, the thermal-gradient-induced migration velocity of thin-film lubricant can be readily predicted using the expressions derived in this paper.

## AUTHOR INFORMATION

### Corresponding Author

\*Tel/Fax: +86-25-84893630. E-mail: wxl@nuaa.edu.cn.

### Notes

The authors declare no competing financial interest.

## ACKNOWLEDGMENTS

We are grateful for the financial support provided by the National Natural Science Foundation of China (no. 51475241), Funding for Outstanding Doctoral Dissertation in NUAU (no. BCXJ15-06), and Funding of Jiangsu Innovation Program for Graduate Education (the Fundamental Research Funds for the Central Universities, no. KYLX\_0239). We are particularly grateful to Professor Harris Wong for the fruitful discussions.

## REFERENCES

- (1) Amiri, M.; Khonsari, M. M. On the thermodynamics of friction and wear—a review. *Entropy* **2010**, *12*, 1021–1049.
- (2) Davis, S. H. Thermocapillary instabilities. *Annu. Rev. Fluid Mech.* **1987**, *19*, 403–435.
- (3) Chaudhury, M. K.; Whitesides, G. M. How to make water run uphill. *Science* **1992**, *256*, 1539–1541.
- (4) Wong, H.; Miksis, M. J.; Voorhees, P. W.; Davis, S. H. Capillarity driven motion of solid film wedges. *Acta Mater.* **1997**, *45*, 2477–2484.

- (5) Daniel, S.; Chaudhury, M. K.; Chen, J. C. Fast drop movements resulting from the phase change on a gradient surface. *Science* **2001**, *291*, 633–636.
- (6) Boi, S.; Martins Afonso, M.; Mazzino, A. Anomalous diffusion of inertial particles in random parallel flows: Theory and numerics face to face. *J. Stat. Mech.: Theory Exp.* **2015**, *2015*, P10023.
- (7) Chaudhury, M. K. Spread the word about nanofluids. *Nature* **2003**, *423*, 131–132.
- (8) Mettu, S.; Chaudhury, M. K. Motion of drops on a surface induced by thermal gradient and vibration. *Langmuir* **2008**, *24*, 10833–10837.
- (9) Wasnik, P. S.; N'Guessan, H. E.; Tadmor, R. Controlling arbitrary humidity without convection. *J. Colloid Interface Sci.* **2015**, *455*, 212–219.
- (10) Chaudhury, M. K.; Chakrabarti, A.; Daniel, S. Generation of motion of drops with interfacial contact. *Langmuir* **2015**, *31*, 9266–9281.
- (11) Khonsari, M. M. A review of thermal effects in hydrodynamic bearings part I: Slider and thrust bearings. *ASLE Trans.* **1987**, *30*, 26–33.
- (12) Cheng, T.; Zhao, B.; Chao, J.; Meeks, S. W.; Velidandea, V. The lubricant migration rate on the hard disk surface. *Tribol. Lett.* **2001**, *9*, 181–185.
- (13) Zhang, J.; Watson, S. J.; Wong, H. Fluid flow and heat transfer in a dual-wet micro heat pipe. *J. Fluid Mech.* **2007**, *589*, 1–31.
- (14) Tadmor, R.; Pepper, K. G. Interfacial tension and spreading coefficient for thin films. *Langmuir* **2008**, *24*, 3185–3190.
- (15) Smith, M. K. Thermocapillary migration of a two-dimensional liquid droplet on a solid surface. *J. Fluid Mech.* **1995**, *294*, 209–230.
- (16) Wong, H.; Miksis, M. J.; Voorhees, P. W.; Davis, S. H. Universal pinch off of rods by capillarity-driven surface diffusion. *Scr. Mater.* **1998**, *39*, 55–60.
- (17) Daniel, S.; Chaudhury, M. K. Rectified motion of liquid drops on gradient surfaces induced by vibration. *Langmuir* **2002**, *18*, 3404–3407.
- (18) Karapetsas, G.; Sahu, K. C.; Sefiane, K.; Matar, O. K. Thermocapillary-driven motion of a sessile drop: Effect of non-monotonic dependence of surface tension on temperature. *Langmuir* **2014**, *30*, 4310–4321.
- (19) Sommers, A. D.; Brest, T. J.; Eid, K. F. Topography-based surface tension gradients to facilitate water droplet movement on laser-etched copper substrates. *Langmuir* **2013**, *29*, 12043–12050.
- (20) Dai, Q. W.; Huang, W.; Wang, X. L. Micro-grooves design to modify the thermo-capillary migration of paraffin oil. *Meccanica* **2016**, DOI: 10.1007/s11012-016-0413-3.
- (21) Dai, Q. W.; Huang, W.; Wang, X. L. A surface texture design to obstruct the liquid migration induced by omnidirectional thermal gradients. *Langmuir* **2015**, *31*, 10154–10160.
- (22) Moumen, N.; Subramanian, R. S.; McLaughlin, J. B. Experiments on the motion of drops on a horizontal solid surface due to a wettability gradient. *Langmuir* **2006**, *22*, 2682–2690.
- (23) Roberts, E. W.; Todd, M. J. Space and vacuum tribology. *Wear* **1990**, *136*, 157–167.
- (24) Huang, W.; Wang, X. L. No migration of ionic liquid under temperature gradient. *Colloids Surf., A* **2016**, *497*, 167–170.
- (25) Tadmor, R. Drops that pull themselves up. *Surf. Sci.* **2014**, *628*, 17–20.
- (26) Greenspan, H. P. On the motion of a small viscous droplet that wets a surface. *J. Fluid Mech.* **1978**, *84*, 125–143.
- (27) Ehrhard, P.; Davis, S. H. Non-isothermal spreading of liquid drops on horizontal plates. *J. Fluid Mech.* **1991**, *229*, 365–388.
- (28) Brochard, F. Motions of droplets on solid surfaces induced by chemical or thermal gradients. *Langmuir* **1989**, *5*, 432–438.
- (29) Brzoska, J. B.; Brochard-Wyart, F.; Rondelez, F. Motions of droplets on hydrophobic model surfaces induced by thermal gradients. *Langmuir* **1993**, *9*, 2220–2224.
- (30) Ford, M. L.; Nadim, A. Thermocapillary migration of an attached drop on a solid surface. *Phys. Fluids* **1994**, *6*, 3183–3185.

- (31) Subramanian, R. S.; Moumen, N.; McLaughlin, J. B. Motion of a drop on a solid surface due to a wettability gradient. *Langmuir* **2005**, *21*, 11844–11849.
- (32) Seeton, C. J. Viscosity–temperature correlation for liquids. *Tribol. Lett.* **2006**, *22*, 67–78.
- (33) Pratap, V.; Moumen, N.; Subramanian, R. S. Thermocapillary motion of a liquid drop on a horizontal solid surface. *Langmuir* **2008**, *24*, 5185–5193.
- (34) Bahadur, P.; Yadav, P. S.; Chaurasia, K.; Leh, A.; Tadmor, R. Chasing drops: Following escaper and pursuer drop couple system. *J. Colloid Interface Sci.* **2009**, *332*, 455–460.
- (35) Tadmor, R. Marangoni flow revisited. *J. Colloid Interface Sci.* **2009**, *332*, 451–454.
- (36) Tadmor, R. Line energy and the relation between advancing, receding, and young contact angles. *Langmuir* **2004**, *20*, 7659–7664.
- (37) Bair, S. The temperature and pressure dependence of viscosity and volume for two reference liquids. *Lubr. Sci.* **2016**, *28*, 81–95.
- (38) Wasan, D. T.; Nikolov, A. D.; Brenner, H. Droplets speeding on surfaces. *Science* **2001**, *291*, 605–606.
- (39) Dai, Q. W.; Huang, W.; Wang, X. L. Surface roughness and orientation effects on the thermo-capillary migration of a droplet of paraffin oil. *Exp. Therm. Fluid Sci.* **2014**, *57*, 200–206.
- (40) Hadland, P. H.; Balasubramaniam, R.; Wozniak, G.; Subramanian, R. S. Thermocapillary migration of bubbles and drops at moderate to large marangoni number and moderate reynolds number in reduced gravity. *Exp. Fluids* **1999**, *26*, 240–248.
- (41) Balasubramaniam, R.; Subramanian, R. S. The migration of a drop in a uniform temperature gradient at large marangoni numbers. *Phys. Fluids* **2000**, *12*, 733.